

Electronic Properties of Alkali- and Alkaline-Earth-Intercalated Silicon Nanowires

S. Sirichantaropass, V. M. García-Suárez,* and C. J. Lambert
Department of Physics, Lancaster University, Lancaster, LA1 4YB, U. K.
(Dated: February 6, 2008)

We present a first-principles study of the electronic properties of silicon clathrate nanowires intercalated with various types of alkali or alkaline-earth atoms. We find that the band structure of the nanowires can be tailored by varying the impurity atom within the nanowire. The electronic character of the resulting systems can vary from metallic to semiconducting with direct band gaps. These properties make the nanowires specially suitable for electrical and optoelectronic applications.

PACS numbers: 73.22.-f, 73.21.Hb, 81.07.Vb

The desire for nanoscale components which integrate gracefully with silicon CMOS technology makes the fabrication and characterization of silicon nanowires particularly attractive. These structures can be grown using a broad range of experimental techniques^{1,2,3,4,5,6} and posses novel properties which may make them suitable as interconnects in very-large-scale integrated devices. Other interesting applications include photoelectronics, since these structures have large direct band-gaps which allow them to work as visible-light emitters with low power consumption. The origin of this change in the band gap is related to quantum confinement^{7,17} which increases the band width and produces an indirect-direct transition as the size of the wire shrinks⁹. The band gap generates a low-voltage gap in the I-V characteristic which is considerably enhanced when the surface is passivated⁸. However, upon doping the gap disappears and the resulting I-V curves display ohmic behavior for low voltages¹³.

Many possible structures for silicon nanowires have been proposed^{3,8,9,14,15,16,17,18,19,20,21}. Those grown from porous silicon are the most stable for diameters down to 1 nm^{9,20,21}. Their structural and cohesive properties are determined by a competition between the highly coordinated core and the surface reconstruction which, due to curvature effects, becomes more important as the nanowire width decreases. There are, however, other types of silicon nanowires with a hollow core and a more coordinated surface which resemble fullerene-like structures. Some of such nanowires can be made sta-

ble by the encapsulation of metallic particles^{10,11,12}, which alter significantly their physical properties and transform the nanowires from semiconducting to metallic. However, pure silicon nanowires derived from the silicon clathrate phases do not need any impurity to be stabilized and are expected to be the most stable for very small diameters^{3,20}. These nanowires can have many different shapes^{8,9,20,21} depending on the basic unit of repetition and the growth direction.

Clathrates are particularly interesting due to their novel elastic²⁵, thermoelectric²⁶, optoelectronic²⁷ and superconducting²⁸ properties. They are grown by nucleating a vapor of silicon or other group IV elements like Ge and Sn around alkali or alkaline-earth atoms generally from the third or bigger rows²². The impurities can be left inside the structure with different concentrations or be removed afterwards. Pristine clathrates are semiconducting and have wider band gaps than the diamond phase of silicon²³, whereas intercalated clathrates are usually metallic²⁴. The most common clathrate lattices have 34 and 46 atoms in the primitive unit cell and are made of Si₂₀ and Si₂₈ cages and Si₂₀ and Si₂₄ cages, respectively.

The smallest of the clathrate-type nanowires are based on the Si₂₀ and Si₂₄ cages^{3,8} and have been predicted to be the most stable configurations in some experiments³. These nanowires are expected to show many of the clathrate properties due to their similarities with the bulk phases. The Si₂₀ cage, which is present in both types of clathrates, is a regular polyhedron made of 12 pentagons. The corresponding nanowire is grown along an axis that passes through two opposite faces (C_{5v} symmetry) and has 30 atoms in the unit cell. The Si₂₄ cage has 12 pentagons and two opposite hexagons. The corresponding nanowire is grown along the direction perpendicular to the hexagons (C_{6v} symmetry) and contains 36 atoms in the unit cell. The transport properties of this nanowire placed between aluminium electrodes and passivated with hydrogen were calculated by Landman and coworkers²⁹ and they found that the nanowire doped with Al atoms was more efficient than the pristine one³⁰. We label these nanowires as Si(30) and Si(36) respectively. The intercalation of alkali or alkaline-earth impurities is made possible by the large endohedral space available inside the cages and the fact that the corresponding bulk structures are stable.

In this article we report ab-initio theoretical studies of the electronic properties of Si(30) and Si(36) nanowires intercalated with the alkali and alkaline-earth metals {Na,K,Rb,Cs}

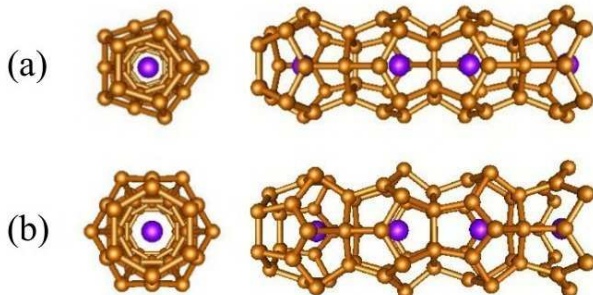


FIG. 1: Top and lateral views of two unit cells of a 2M@Si(30) (a) and a 2M@Si(36) (b), where M is an alkali or alkaline-earth atom.

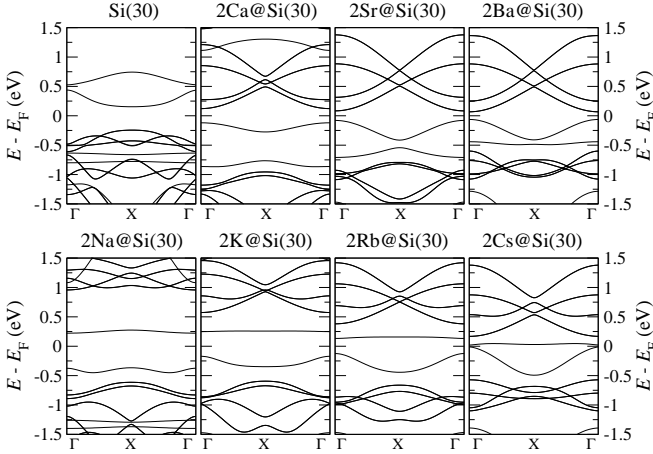


FIG. 2: Band structure of pristine (first top box), alkaline-earth intercalated (next three top boxes) and alkali intercalated (bottom) Si(30) nanowires.

and $\{\text{Ca},\text{Sr},\text{Ba}\}$, respectively, which correspond to typical clathrate intercalations²². We label them as $2\text{M}@Si(30)$ and $2\text{M}@Si(36)$, where 2M represents the two alkali or alkaline earth atoms included in the unit cell. An example of the top and lateral views of these structures can be seen in Fig. (1). We predict that intercalation alters dramatically the electronic structure of the nanowires and allows one to tailor their electronic properties. The overall changes can be traced back to three different effects: structural deformation, hybridization and charge transfer from the endohedral impurity. As a consequence, the electronic character of the nanowires can range from metallic to semiconducting. The band gaps in the latter are usually direct and comparable to the band gap of bulk silicon, which make these nanowires particularly useful for optoelectronics applications in the infrared or visible range.

The electronic structure was calculated with the SIESTA code³², which is based on density functional theory³¹ and employs norm-conserving pseudopotentials and linear combinations of atomic orbitals. The valence states were spanned with optimized double- ζ polarized basis sets. In the heaviest atoms (K,Ca,Rb,Sr,Cs,Ba) we included relativistic corrections in the pseudopotentials and semicore states in the basis set. The exchange and correlation energy and potential were evaluated with the local density approximation (LDA). All atomic coordinates and the lattice were fully relaxed until all the forces and the stress were smaller than 0.02 eV/Å and 1.0 GPa, respectively. The dimensions of the unit cell along the perpendicular directions were made large enough to avoid overlaps and electrostatic interactions with other images. The real space grid was defined with a plane wave cutoff of 200 Ry. The Brillouin zone along the nanowire growth direction was sampled with 30 k -points to perform the structural relaxations and 200 k -points to calculate the densities of states (DOS), where a broadening parameter of 0.01 eV was used. The binding energies were computed by removing the basis set superposition error³³ which comes from the localized character of the basis functions.

First we focus on the pristine nanowires, whose initial un-

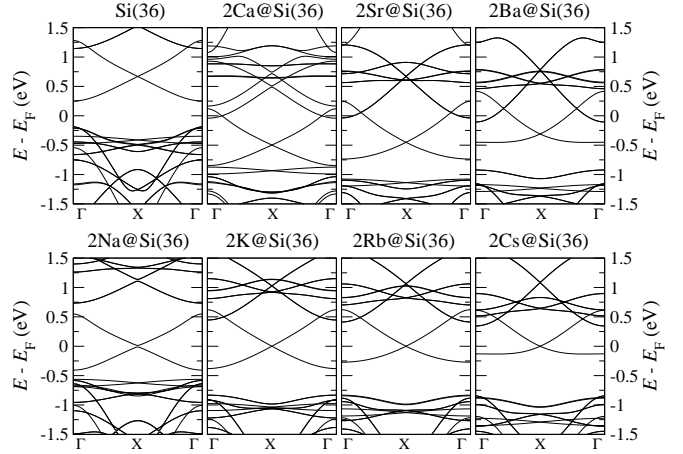


FIG. 3: Band structure of pristine (first top box), alkaline-earth intercalated (next three top boxes) and alkali intercalated (bottom) Si(36) nanowires.

relaxed configuration corresponds to that of the ideal polyhedral structures. Upon full relaxation the structure changes slightly and compresses, resulting in lattice constants along the growth direction of 10.50 Å and 10.28 Å for the Si(30) and Si(36), respectively. The cohesive energies of both nanowires are very similar, as can be seen in Table I, but the Si(36) is slightly more stable³, which is probably due to the fact that in this nanowire the presence of sixfold rings generates bond angles much closer to the ideal bond angles of diamond silicon and reduces the strain of the structure. The electronic band structures computed for the pristine Si(30) and Si(36) nanowires are shown in the first boxes of Figs. (2) and (3), respectively. The Si(30) nanowire has a clear direct band gap at the X point with a LDA value of 0.40 eV. Taking into account that the LDA underestimates bands gaps, but gives correct relative orders and trends, the previous result would imply, after a scissor-correction of 0.7 eV, which is usually employed in silicon²³, a true band gap of ~ 1.10 eV³⁴, similar to the band gap of diamond silicon. The Si(36) nanowire has also a direct band gap, with a width of 0.44 eV³⁸, but it is located at Γ instead of X. The scissor correction gives in this case a value of 1.14 eV. The character and width of such band gaps, which lie close to the low visible energy range, make these nanowires perfect candidates for light emitting devices in optoelectronic applications on the nanoscale.

When the impurity atoms are inserted in the structure the lattice undergoes a small deformation and expands. The changes in the mean atomic distances and in the lattice vector along the growth direction are in general smaller than a 5%. In table I we also show the magnitude of the band gaps and the binding energy of the intercalated nanowires. All these structures are exothermic, except for $2\text{Cs}@Si(30)$, which is slightly endothermic³⁹. Inspection of the binding energies shows three clear trends. First, the Si(30) nanowires are always less stable than the Si(36) due to the unfavorable interaction produced by the strong compression in the small Si(30) cages. Second, the alkali intercalations are always less stable than the alkaline-earth because the radii of the alkali elements

TABLE I: Binding energies (BE) and band gaps (BG) of pristine and alkali- or alkaline-earth intercalated Si(30) and Si(36) nanowires.

	Si(30)		Si(36)	
	BE (eV)	BG (eV)	BE (eV)	BG(eV)
Pristine	-5.22	0.40	-5.25	0.44
Na	-2.25	0.60	-2.42	0.03
K	-1.40	0.42	-2.47	0.00
Rb	-0.72	0.26	-2.37	0.00
Cs	0.42	0.03	-2.08	0.00
Ca	-3.70	0.24	-4.88	0.00
Sr	-3.86	0.16	-4.52	0.00
Ba	-4.33	0.13	-5.67	0.00

are larger than those of the corresponding alkaline-earth and this again increases the possibility of unfavorable interactions. Third, in the alkali atoms bigger than sodium the binding energy decreases as the atomic radius increases whereas in the alkaline-earth the trend is just the opposite, with the exception of 2Sr@Si(36). These apparently contradictory behaviors can be again understood in terms of the bigger size of the alkali impurities as compared to the alkaline-earth impurities and the fact that the latter elements donate more charge to the silicon lattice, which stabilizes the structure²⁶ and increases the bonding with the positive ion.

The band structures of the intercalated nanowires are plotted in Figs. (2) and (3). In the Si(30) structures, all nanowires have a direct band gap at Γ . The only exception to this rule is that corresponding to the lightest element, 2Na@Si(30), where the band gap is indirect, although it is difficult to say due to the small difference between both maxima of the top of the valence band. Moving to the bottom of the periodic table, the band gap gradually decreases towards Cs and Ba. This is due to the growing separation in energy between the outer levels of the impurities and the silicon network levels which decreases the interaction between them. It is interesting to note that in the alkali atoms the magnitude of the gap is reduced by the presence of a low-dispersive state located just above the Fermi level, whereas in the alkaline-earth elements the lowest conduction bands are very dispersive. Such features, like the existence of gaps and low dispersive bands, would have important consequences in the transport properties of these systems, giving rise to interesting effects like negative differential resistance. In the Si(36) structures the general situation is rather different. Due to the larger size of the Si(36) cages and the corresponding smaller interaction of the metallic atoms with the silicon structure, the bands of the filled nanowires resemble more closely those of the empty ones. For example, in 2K@Si(36), 2Rb@Si(36) and 2Cs@Si(36) the only effect seems to be a rigid downwards shift of the whole silicon band structure. These intercalations give rise to a metallic or semi-metallic behavior, where two bands cross at the Fermi level or open a small band gap. The same behavior is found for all the alkaline-earth intercalations.

The above properties can be understood by dividing the effect of the impurities into three parts: a structural deformation and two purely electronic effects associated with charge

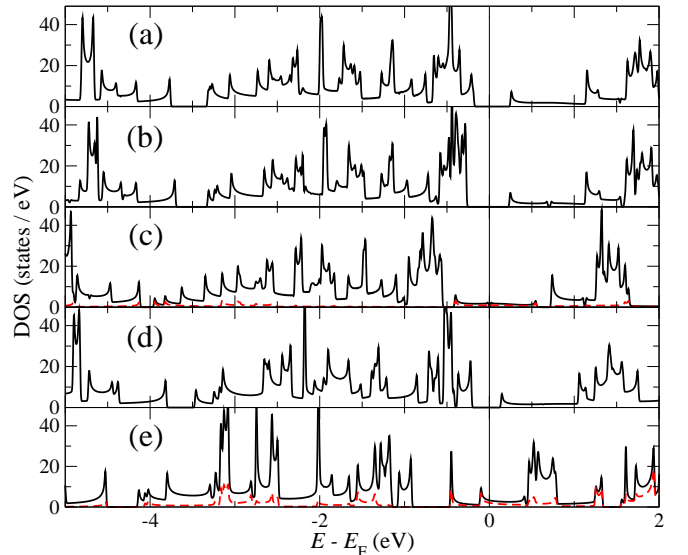


FIG. 4: Projected density of states on the silicon atoms of a pristine Si(36) (a), a Na-deformed pristine Si(36) (b), a 2Na@Si(36) (c), a Ba-deformed pristine Si(36) (d) and a 2Ba@Si(36) (e). The dashed lines in graphs (c) and (e) are the projected densities of states on the sodium and barium atoms, respectively, multiplied by a factor of 3 for clarity.

transfer and hybridization. The effect of the structural deformation can be clearly determined by comparing the electronic structure of a relaxed pristine clathrate with the electronic structure of a pristine clathrate in the structural configuration of the intercalated system. We show in Fig. (4) the density of states of the pristine Si(36) nanowire and two typical intercalations corresponding to the most studied intercalated clathrates, i. e. those with sodium and barium²⁴. Box (a) corresponds to the pristine and relaxed nanowire, (b) and (d) to the pristine nanowire in the structure of the Na- and Ba-intercalated systems, respectively, and (c) and (e) to the corresponding intercalated nanowires. As can be seen by comparing graphs (a) with (b) or (d), structural modifications are more pronounced in the barium encapsulation due to the larger size of this element. In general, the bigger the atom, the larger the modification it produces on the silicon network. The same behavior is found for the Si(30) nanowires, but due to the smaller endohedral space of the Si₂₀ cages and therefore the larger deformation produced by the impurity, the changes are more dramatic. These structural-induced changes in the electronic properties can be understood in terms of the increase or, in some cases, decrease of the distance between neighbor atoms, which reduce or increase the couplings and therefore the bandwidths. The final outcome of the structural deformations is then mainly a modification of the size of the band gaps and widths. In some cases, modification of the bond angles can also move states downwards or upwards depending on whether or not they approach the ideal angles of the sp^3 bonding. This is specially relevant in the Si(30) nanowires.

The effect of the charge transfer can be easily demonstrated by comparing the electronic band structures of the intercalated

systems with the pristine ones. Since alkali and alkaline-earth atoms are very electropositive elements, their electronic levels are well above those of silicon and tend to donate the outer one (in the alkali) or two (in the alkaline-earth) electrons to the silicon network. This can be clearly seen in Figs. (2) and (3), where one or two silicon bands move below the Fermi level in the alkali or alkaline-earth intercalations, respectively. Note that since the bands are not spin-split, the number of electrons transferred per unit cell is 2 in the former elements and 4 in the latter, coming from the two atoms in the unit cell.

The hybridization between silicon states and impurity states can be determined by examining the electronic density of states of Fig. (4). As expected, large-diameter elements, such as Ba, interact more strongly with the cage and produce greater hybridization. This significantly modifies the electronic structure of the intercalated system, compared to that of the isostructural system without the impurity, at the energies where the bands of the endohedral atom are located, as can be easily deduced by looking at the projected density of states on the barium atoms. As a consequence of the presence or absence of hybridization for heavy or light elements, respectively, we conclude that the bond between the bigger impurities and the silicon network in the Si(36), and to a greater extent in the Si(30), has some covalent character but becomes increasingly ionic as the size of the atom decreases⁴⁰.

In summary, we have found that the combination of structural deformation, charge transfer and hybridization in alkali or alkaline-earth intercalated silicon clathrate nanowires produces a rich behavior that allows one to tailor these systems for technological applications. Their electronic character ranges from semiconducting to metallic, which makes them suitable to act as interconnects for nanocircuits or as other types of electronic elements. Furthermore, the character and width of the band gaps, which in most cases are direct and close to the visible, promise important optoelectronic applications. Finally, the resemblance of these systems to the clathrate bulk phases suggests that superconductivity and novel thermoelectric or elastic properties may be fruitful avenues for future investigations.

Acknowledgments

We acknowledge financial support from the European Commission and the British EPSRC, DTI, Royal Society, and NWDA. VMGS thanks Jaime Ferrer for useful discussions and the EU network MRTN-CT-2004-504574 for a Marie Curie grant.

* Electronic address: v.garcia-suarez@lancaster.ac.uk

¹ Y. F. Zhang, Y. H. Tang, N. Wang, D. P. Yu, C. S. Lee, I. Bello, and S. T. Lee, *Appl. Phys. Lett.* **72**, 1835 (1998).

² A. M. Morales and C. M. Lieber, *Science* **279**, 208 (1998).

³ B. Marsen and K. Sattler, *Phys. Rev. B* **60**, 11593 (1999).

⁴ J. L. Gole, J. D. Stout, W. L. Rauch, and Z. L. Wang, *Appl. Phys. Lett.* **76**, 2346 (2000).

⁵ J. D. Holmes, K. P. Johnston, R. C. Doty and B. A. Korgel, *Science* **287**, 1471 (2000).

⁶ D. D. D. Ma, C. S. Lee, F. C. K. Au S. Y. Tong, and S. T. Lee, *Science* **299**, 1874 (2003).

⁷ R.-P. Wang, G.-W. Zhou, Y.-L. Liu, S.-H. Pan, H.-Z. Zhang, D.-P. Yu, and Z. Zhang, *Phys. Rev. B* **61**, 16827 (2000).

⁸ M. Durandurdu, *Phys. Stat. Sol B*, **243**, R7 (2006).

⁹ I. Ponomareva, M. Menon, E. Richter, and A. N. Andriotis, *Phys. Rev. B* **74**, 125311 (2006).

¹⁰ A. N. Andriotis, G. Mpourmpakis, G. E. Froudakis, and M. Menon, *New J. Phys.* **4**, 78 (2002).

¹¹ A. K. Singh, T. M. Briere, V. Kumar, and Y. Kawazoe, *Phys. Rev. Lett.* **91**, 146802 (2003).

¹² A. K. Singh, V. Kumar, and Y. Kawazoe, *J. Mater. Chem.* **14**, 555 (2004).

¹³ G. Zheng, W. Lu, S. Jin, and C. M. Lieber, *Adv. Mater. (Weinheim, Ger.)* **16**, 1890 (2004).

¹⁴ M. Menon and E. Richter, *Phys. Rev. Lett.* **83**, 792 (1999).

¹⁵ B.-X. Li, P.-L. Cao, R. Q. Zhang, and S. T. Lee, *Phys. Rev. B* **65**, 125305 (2002).

¹⁶ Y. Zhao and B. I. Yacobson, *Phys. Rev. Lett.* **91**, 035501 (2003).

¹⁷ X. Zhao, C. M. Wei, L. Yang, and M. Y. Chou, *Phys. Rev. Lett.* **92**, 236805 (2004).

¹⁸ M. Menon, D. Srivastava, I. Ponomareva, and L. A. Chernozatonskii, *Phys. Rev. B* **70**, 125313 (2004).

¹⁹ R. Rurrali and N. Lorente, *Phys. Rev. Lett.* **94**, 026805 (2005).

²⁰ R. Kagimura, R. W. Nunes, and H. Chacham, *Phys. Rev. Lett.* **95**, 115502 (2005).

²¹ I. Ponomareva, M. Menon, D. Srivastava, and A. N. Andriotis, *Phys. Rev. Lett.* **95**, 265502 (2005).

²² A. San-Miguel and P. Toulemonde, *High Pressure Research* **25**, 159 (2005).

²³ G. B. Adams, M. O'Keeffe, A. A. Demkov, O. F. Sankey, and Y.-M. Huang, *Phys. Rev. B* **49**, 8048 (1994).

²⁴ K. Moriguchi, M. Yonemura, A. Shintani, and S. Yamanaka, *Phys. Rev. B* **61**, 9859 (2000).

²⁵ A. San-Miguel, P. Kéghélian, X. Blase, P. Mélinon, A. Perez, J. P. Itié, A. Polian, E. Reny, C. Cros, and M. Pouchard, *Phys. Rev. Lett.* **83**, 5290 (1999).

²⁶ J. S. Tse, K. Uehara, R. Rousseau, A. Ker, C. I. Ratcliffe, M. A. White, and G. MacKay, *Phys. Rev. Lett.* **85**, 114 (2000).

²⁷ J. Gryko, P. F. McMillan, R. F. Marzke, G. K. Ramachandran, D. Patton, S. K. Deb, and O. F. Sankey, *Phys. Rev. B* **62**, R7707 (2000).

²⁸ H. Kawaji, H. O. Horie, S. Yamanaka, and M. Ishikawa, *Phys. Rev. Lett.* **74**, 1427 (1995).

²⁹ U. Landman, R. N. Barnett, A. G. Scherbakov, and P. Avouris, *Phys. Rev. Lett.* **85**, 1958 (2000).

³⁰ We would like to emphasize that our work deals with infinite nanowires. In general the attachment to an electrode will decrease the transmission and/or kill some of the conductance channels, but it is difficult to say up to what extent because there are many details that have to be taken into account (type of electrodes, contact geometry, wire length, etc.). A full ab-initio calculation for each of the nanowires similar to that of Landman *et al.*²⁹ would be needed to clarify this point.

³¹ W. Kohn and L. J. Sham, *Phys. Rev.* **140**, A1133 (1965).

³² J. M. Soler, E. Artacho, J. D. Gale, A. García, J. Junquera, P. Ordejón, and D. Sánchez-Portal, *J. Phys.: Condens. Matter* **14**, 2745 (2002).

³³ S. F. Boys and F. Bernardi, *Mol. Phys.* **19**, 553 (1970).

³⁴ There are other methods that are known to improve the energy gap and give quasiparticle energies close to experiments, like the GW self-energy method³⁵, self interaction corrections³⁶, and the LDA+U method³⁷. The application of some of these approaches to silicon nanowires will be the topic of future investigations.

³⁵ M. S. Hybertsen and S. G. Louie, *Phys. Rev. B* **34**, 5390 (1986).

³⁶ J.P. Perdew and A. Zunger, *Phys. Rev. B* **23**, 5048 (1981).

³⁷ I. Anisimov, F. Aryasetiawan, and A. I. Lichtenstein, *J. Phys.: Condens. Matter* **9**, 767 (1997).

³⁸ The LDA values are larger but comparable to those found recently by Durandurdu⁸ using GGA.

³⁹ Since the LDA tends to overestimate the binding energies we do not exclude the possibility that some of the less exothermic compounds, like 2K@Si(30) and 2Rb@Si(30), could be slightly endothermic.

⁴⁰ The hybridization and the prevalence of covalent or ionic character can also be determined by looking at the charge density around the metallic impurities²⁴, i. e. if the charge is smoothed out it means that the bond is stronger and has a larger covalent character, whereas if the charge is strongly localized around the impurity the bond is mainly ionic.